Vol. 25, No. 3(2026) Bio26844

Revista Mexicana de Ingeniería Química

Effect of dextrose concentration on melanin-mediated immobilization of CuO nanoparticles by *Cladosporium* sp.

Efecto de la concentración de dextrosa en la inmovilización mediada por melanina de nanopartículas de CuO por *Cladosporium* sp.

M. Contla-Ubaldo[1], M. García-Rivero[2], N. Velasco-Alvarez[1], T. Volke-Sepúlveda[1]*

[1]Department of Biotechnology, Universidad Autónoma Metropolitana-Iztapalapa. Av. Ferrocarril San Rafael Atlixco 186, Col. Leyes de Reforma 1A Sección, Iztapalapa, 09310, Mexico City, MEXICO.
[2]Division of Chemical and Biochemical Engineering, TecNM/Tecnológico de Estudios Superiores de Ecatepec. Av. Tecnológico s/n, Valle de Anahuac, 55210 Ecatepec, State of Mexico, MEXICO.

Received: April 8, 2026; Accepted: September 1, 2026

Abstract

The increasing use of copper oxide nanoparticles (CuO-NPs) in industry and their improper environmental release have raised concerns regarding soil toxicity. Various microorganisms, particularly dark septate endophytes (DSE) fungi, possess specialized mechanisms to tolerate metallic pollutants, including melanin-mediated immobilization and antioxidant defense systems. This study aimed to determine the effect of dextrose concentration on melanin production and evaluate its relationship with tolerance and the antioxidant response of the DSE fungus *Cladosporium* sp. UAM12 exposed to CuO-NPs (~50 nm). Using a central composite design (CCD), the effects of CuO-NP and dextrose concentration on biomass production, melanin synthesis, and copper sorption were analyzed. Melanin synthesis was optimized at 60 g L^{-1} dextrose and 160 mg L^{-1} CuO-NPs. High dextrose levels increased biomass production but reduced fungal tolerance to CuO-NPs. After 14 days, CuO-NPs did not significantly affect the biomass yield (Y_{XS}), but delayed dextrose consumption between 2 and 12 days. DOPA-melanin production showed a significant positive correlation with copper sorption, with approximately 80% of the total copper in biomass being sequestered in the cell wall. Increased activity of superoxide dismutase and peroxidases contributed to mitigating CuO-NP-induced oxidative stress. These findings contribute to understanding some biochemical strategies of *Cladosporium* sp. UAM12 to resist the toxicity of CuO-NPs, highlighting its potential for use in bioremediation processes in matrices contaminated with metallic NPs.

Keywords: dark septate endophytic fungi, copper sorption, oxidative stress, antioxidant defense.

Resumen

El uso creciente de nanopartículas de óxido de cobre (NP-CuO) en la industria y su disposición inadecuada al ambiente han generado preocupaciones respecto a la toxicidad del suelo. Diversos microorganismos, particularmente los hongos endófitos septados oscuros (DSE), tienen mecanismos especializados para tolerar contaminantes metálicos, incluyendo la inmovilización mediada por melanina y los sistemas de defensa antioxidante. Este estudio tuvo como objetivo determinar el efecto de la concentración de dextrosa en la producción de melanina y evaluar su relación con la tolerancia y la respuesta antioxidante del hongo DSE *Cladosporium* sp. UAM12 expuesto a NP-CuO (~50 nm). Utilizando un diseño compuesto central (DCC), se analizaron los efectos de la concentración de NP-CuO y de dextrosa sobre la producción de biomasa, la síntesis de melanina y la sorción de cobre. La síntesis de melanina se optimizó con 60 g L^{-1} de dextrosa y 160 mg L^{-1} de NP-CuO. La alta concentración de dextrosa aumentó la producción de biomasa, pero redujo la tolerancia del hongo a las NP-CuO. Después de 14 días, las NP-CuO no afectaron significativamente el rendimiento celular (Y_{XS}), pero retrasaron el consumo de dextrosa entre 2 y 12 días. La producción de DOPA-melanina tuvo una correlación positiva y significativa con la sorción de cobre, encontrando cerca del 80% del cobre total en biomasa secuestrado en la pared celular. El aumento en la actividad superóxido dismutasa y peroxidasa contribuyó a mitigar el estrés oxidativo inducido por las NP-CuO. Estos hallazgos contribuyen a comprender algunas estrategias bioquímicas en *Cladosporium* sp. UAM12 para resistir la toxicidad de las NP-CuO, destacando su potencial para su uso en procesos de biorremediación de matrices contaminadas con NPs metálicas.

Palabras clave: hongos endófitos septados oscuros, sorción de cobre, estrés oxidativo, defensa antioxidante.

* *Corresponding author. E-mail*: tvs@xanum.uam.mx;
https://doi.org/10.24275/rmiq/Bio26844
ISSN:1665-2738, *issn-e*: 2395-8472

1 Introduction

Nanoparticles (NPs), characterized by their size smaller than 100 nm, exhibit unique physicochemical properties that make them useful across many fields, including environmental remediation, medicine, electronics, and agriculture. Copper NPs have gained particular interest because, in addition to being cost-effective and readily available, they are versatile, offer excellent electrical conductivity, and are compatible with diverse materials (Saleem *et al*., 2024). Copper oxide NPs (CuO-NPs) are especially used in agriculture, where they are applied in fertilizers and pesticides. Due to their widespread use, toxicity is a major concern associated with the indiscriminate application of NPs in agriculture, which, along with the risk of accumulation in the soil, makes them an environmental contaminant. Global production of CuO-NPs was estimated at about 1600 tons in 2025, with roughly 36 tons ending up in the soil (Tripathi *et al*., 2024).

Although copper is an essential micronutrient, the release of CuO-NPs nanoparticles into soil and other environmental matrices can become toxic at high concentrations by inducing oxidative stress (Tripathi *et al*., 2024). Soil microorganisms, including bacteria and fungi, play key roles in helping plants tolerate abiotic stress. Particularly, fungi have remarkable mechanisms for metal detoxification that include biosorption, intracellular sequestration, exclusion, and active transport (Kumar *et al*., 2015; Khan *et al*., 2019). Dark septate endophytes (DSE) are a diverse group of root-associated fungi commonly found in plants exposed to stressful conditions such as drought, salinity, and heavy metal (HM) contamination (Malicka *et al*., 2022). The dark pigmentation of their mycelium results from the melanin accumulation in the cell wall, with DHN-melanin (1,8-dihydroxynaphthalene) and DOPA-melanin (L-3,4-dihydroxyphenylalanine) being the two main types (Malicka *et al*., 2022; Suthar *et al*., 2023). Melanins are polymers of extremely complex structure, formed by heterologous polyaromatic compounds of indoles or polyphenols (Yu *et al*., 2026). Most DSE have both melanin-dependent and melanin-independent HM-detoxification mechanisms, including cell wall immobilization, intracellular complexation and compartmentalization, reactive oxygen species (ROS) scavenging, and extracellular metal efflux (Malicka *et al*., 2022). However, intracellular accumulation of HMs inevitably triggers excessive ROS production, resulting in oxidative stress that alters metabolism, damages biomolecules (proteins, lipids, and DNA), and can lead to programmed cell death. Consequently, oxidative stress is considered a primary driver of HM-induced cell death in microorganisms (Lu *et al*., 2021; Priyadarshini *et al*., 2021). To counteract the ROS-induced damage, many DSE fungi possess efficient antioxidant systems composed of enzymatic and non-enzymatic components that together regulate intracellular ROS levels (Ban *et al*., 2023). Melanin-dependent processes further enhance tolerance by reducing free metal ion concentrations in the vicinity of hyphae, supporting growth under high HM levels and providing an extracellular detoxification barrier that limits metal uptake into cells (Potisek *et al*., 2021). Melanin effectively reduces the bioavailability of metal ions by binding them through the diverse functional groups present in its heterocyclic rings (Ban *et al*., 2023; Suthar *et al*., 2023). Its chemical structure enables the stabilization of free radicals and unpaired electrons, leading to the neutralization of excess reactive oxygen species (ROS) induced by heavy metal exposure, thereby mitigating the oxidative stress associated with intracellular accumulation (Singh *et al*., 2021).

In general, a correlation has been observed between high melanin content and antioxidant activity in DSE fungi, resulting in increased tolerance to heavy metals (Ban *et al*., 2012; Zhan *et al*., 2011). The most important factor in improving melanin production in DSE fungi is the choice of carbon and nitrogen sources. Organic nitrogen sources (such as peptones) are better than inorganic ones because, in addition to nitrogen, they provide peptides and amino acids that are precursors or inducers of melanin synthesis. Likewise, the concentration of the carbon source plays a fundamental role in regulating fungal metabolism by providing the energy necessary for the synthesis of precursors involved in the metabolic pathways associated with melanin biosynthesis (Yu *et al*., 2026). In melanized fungi, the main precursors include tyrosine derivatives and L-DOPA, involved in the synthesis of DOPA-melanin, as well as acetyl-CoA intermediates associated with the formation of DHN-melanin (Lin and Xu, 2023). Thus, the availability of a carbon source provides the metabolic resources necessary for the activation of these biosynthetic pathways. For instance, for large-scale melanin production by *Auricularia auricula*, glucose, tyrosine, peptone, and $CaCO_3$ significantly increased production (Sun *et al*., 2016). In another study with *Aspergillus nidulans*, an increase in glucose concentration (1.62%) and the use of vinasse (0.81%) significantly improved (more than twofold) melanin production (Campanhol *et al*., 2023).

Among DSE, *Cladosporium* species frequently colonize roots, enhance plant stress tolerance, and have been applied for biosorption of azo dyes (Jimenez-Gonzalez *et al*. 2024), as well as in phyto- and bioremediation of HMs and metallic NPs (Ban *et al*., 2012; Răut *et al*., 2021). These fungi can

help sequester metals in root cell walls as insoluble complexes, thereby limiting translocation to aerial tissues (Malicka *et al*., 2022). However, the precise role of melanin in this protective process remains incompletely understood (Ban *et al*., 2012; Berthelot *et al*., 2020), highlighting the need for further research on the biochemical properties and metal-binding capacity of fungal melanin.

In this context, we hypothesize that increased dextrose concentration improves melanin synthesis in *Cladosporium* sp., thereby strengthening its antioxidant defense system and improving tolerance to CuO-NPs-induced stress. Thus, the study aimed to assess the influence of dextrose concentration in melanin production and its relationship with CuO-NPs tolerance and antioxidant enzyme activity in *Cladosporium* sp. For this purpose, we measured melanin production, copper bioaccumulation, and antioxidant enzyme activity over time under a range of CuO-NPs concentrations to assess the potential of DSE fungi for bioremediation of matrices contaminated with metal nanoparticles.

2 Methods and materials

2.1 Microorganism

The DSE fungus *Cladosporium* sp. UAM12 was isolated from *Dodonaea viscosa* seedlings cultivated in vitro in Murashige-Skoog (MS) medium and is therefore considered as an endophyte of this shrub. The strain was preserved on potato dextrose agar (PDA) medium at 4°C, molecularly identified, and deposited in the Biological Control Department Collection (SENASICA, Mexico).

2.2 Central composite design (CCD)

The effect of the initial concentration of dextrose (G-0922685, Meyer) and CuO-NPs (<50 nm, 544868, Sigma-Aldrich) on biomass and melanin production, and Cu sorption in the mycelium was evaluated using a central composite design (CCD) in Sabouraud medium (VM1043038-312, Microbiology). Dextrose and CuO-NP concentrations were tested within the ranges of 11.7–68.3 g L^{-1} and 15–300 mg L^{-1}, respectively. For incorporation into the medium, CuO-NPs were dispersed in distilled water (1 g L^{-1}) and sonicated at 305 W for 15 min at 25 °C (SOLTEC). An aliquot of the suspension corresponding to the final concentration was added to the culture medium prior to sterilization (15 psi, 120 °C). All experiments were done in triplicate. The coded independent variables and their real values are shown in Table S1. The results of the CCD allowed us to draw the following quadratic model (Eq. 1):

$$y = \beta_0 + \beta_{x1} + \beta_{x2} + \beta_{x1x2} + \beta_{x1}^2 + \beta_{x2}^2 \quad (1)$$

Where y is the predictive response according to the model, β_0 corresponds to the intercept coefficient, β_{x1} y β_{x2} are the coefficients of the linear effect, β_{x1x2} is the interaction coefficient and β_{x1}^2 β_{x2}^2 are the coefficients of the quadratic effect; x_1 and x_2 are the coded values for dextrose and CuO-NPs, respectively.

2.3 Kinetic assays

To analyze the interaction between the fungus and CuO-NPs under the conditions identified by the CCD, kinetic tests of biomass and melanin production, as well as dextrose consumption, were performed. For this, the strain was inoculated (1.68 x 10^4 spores cm^{-2}) on the surface of Petri dishes with modified Sabouraud medium (with a total dextrose concentration of 60 g L^{-1}) with or without CuO-NPs (160 mg L^{-1}). The assays were conducted in triplicate for 14 days (27 ºC), taking a sample (0.95 cm^2 disks) from each dish every 48 h.

The specific growth rate (μ) was estimated using Eq. 2, using data corresponding to the first 10 days of culture, since growth was no longer exponential after this period.

$$\ln\left(\frac{B}{Bo}\right) = \mu \cdot (t - t_0) \quad (2)$$

Where B is the fungal biomass quantified in dry weight (DW); t_0 and t are the times at which exponential growth begins and ends, respectively. By performing a linear regression of the growth data, expressed in terms of $ln\ (B/B_0)$ vs. $(t - t_0)$, the value of μ corresponds to the slope of the straight line during the exponential phase (2 to 10 days). The doubling time (t_d) was estimated from the μ values obtained for each condition using the relationship $t_d = ln\ (2)/\mu$. Cell yield (Yxs) was estimated by relating the biomass produced (ΔX) to the dextrose consumed (ΔS) at the final time of the culture (14 days).

2.4 Analytical methods

2.4.1 Biomass

Fresh biomass from each Petri dish was removed with a spatula, suspended in 50 mL of distilled water, and heated at 100 °C for 10 min to remove residual culture medium. The biomass was then filtered through a cellulose filter (11 μm, Whatman), oven-dried at 60 °C for 24 h (WTC, Binder), and weighed to determine the biomass dry weight. Fungal tolerance to CuO-NPs was assessed by calculating the mean inhibitory concentration (IC_{50}), defined as the CuO-NP concentration that inhibits 50% of mycelial growth (Ban *et al*., 2012).

Cell defragmentation was performed to separate the cell wall from the hyphae (Zhan *et al*., 2015). Biomass was removed from the culture medium, and the fresh weight (FW) was recorded. For each assay, 100 mg of fresh biomass was mixed with 20 mL of extraction buffer containing 1 mM DL-dithiothreitol, 50 mM Tris-HCl (pH 7.5), and 0.25 M sucrose. The suspension was centrifuged at 3000 rpm for 15 min (5810-R, Eppendorf), and the resulting pellet (cell wall fraction) was microwave-digested for subsequent copper quantification.

2.4.2 *Dextrose consumption*

Dextrose concentration was determined using the phenol–sulfuric acid method (DuBois *et al*., 1956). A sample of biomass-free culture medium (the volume corresponding to a 0.95 cm^2 disc) was melted in a water bath (10 min, 100 °C). Then, 2 mL of the sample were mixed with 1 mL of 5% (w/v) phenol solution and 5 mL of concentrated H_2SO_4. The reaction mixture was allowed to stand at room temperature for 20 min. Total sugar concentration was quantified spectrophotometrically at 480 nm (UV-VIS 1900i, Shimadzu), using dextrose (0–10 mg L^{-1}) as the calibration standard.

2.4.3 *Copper in biomass*

About 100 mg of dried fungal biomass (60°C, 24 h) were completely digested (200°C, 15 min) in a closed-vessel microwave digestion system (MARSXpress, CEM) using a mixture (5:4 v/v) of 69% HNO_3 (Instra-Analyzed, J.T. Baker) and deionized (DI) water (18 MΩ cm^{-1}, PureLab-Q Elga). The digested samples were filtered through 0.45 μm cellulose filters (Whatman), and the final volume was adjusted to 10 mL with DI water. Total Cu content in the biomass was determined by flame–atomic absorption spectrometry (AA-6300, Shimadzu) at 324.8 nm using an air–acetylene flame. Standard curves (0–10 μg mL^{-1}) were prepared from a Cu standard solution (1000 μg mL^{-1}, Hycel) diluted in 1% HNO_3. To determine the solubilization rate of the copper contained in the CuO-NPs (160 mg L^{-1}), the concentration of dissolved Cu in an abiotic control of the culture medium was analyzed.

2.4.4 *Analysis of the type of melanin produced*

To determine the type of melanin produced by the fungus, kojic acid (K3125, Sigma-Aldrich) and tricyclazole (45808, Supelco) were used as melanin inhibitors. Kojic acid was dissolved in distilled water and incorporated into the culture medium prior to sterilization to achieve a final concentration of 3 g L^{-1}. A solution of tricyclazole (1 g L^{-1}) was prepared in 96% ethanol and added to the sterile culture medium to obtain a final concentration of 50 mg L^{-1}.

For the assay, a conidial suspension of *Cladosporium* sp. (1.68×10^4 spores per cm^2) was inoculated on the surface of Petri dishes containing modified Sabouraud medium, either without or with CuO-NPs (160 mg L^{-1}). Cultures were incubated at 27 °C for 14 days, in triplicate. The resulting biomass from each condition was quantified in DW and processed for melanin content analysis.

2.4.5 *Melanin extraction and purification*

To extract melanin, about 100 mg of fresh biomass was boiled in distilled water (50 mL) for 10 min to remove residual culture medium. The sample was then oven-dried (60°C, 24 h), and its dry weight was recorded (Beltrán-García *et al*., 2014). The dried biomass was treated with 2 M NaOH (100ºC, 3 h) in a digestion block (DRB200, Hach). The resulting mixture was filtered through a cellulose filter (11 μm, Whatman), and the filtrate was acidified with 3 M HCl (X45D16, Macron) to pH 2. The precipitated melanin was collected by centrifugation (5000 rpm, 20 min) and purified by acid hydrolysis with 6 M HCl (100 ºC, 2 h) to remove residual carbohydrates and proteins. The obtained precipitate was centrifuged again (5000 rpm, 20 min) and washed with a 1:10 (v/v) mixture of ethanol (96%) and chloroform (Reagent Grade, J.T. Baker) to remove lipids, followed by washing with distilled water and an additional centrifugation step (5000 rpm, 15 min). The purified melanin was oven-dried (60°C, 24 h), dissolved in 0.1 M NaOH, and its absorbance was measured spectrophotometrically at 400 nm. Quantification was performed using a standard curve (0–170 μg mL^{-1}) prepared with synthetic melanin (M8631, Sigma-Aldrich).

2.4.6 *Antioxidant activity*

To evaluate the effect of CuO-NPs on the fungal antioxidant capacity, the activity of antioxidant enzymes —catalase, peroxidases, and superoxide dismutase— was determined. For enzyme activity analyses, the fungus was inoculated onto the culture medium overlaid with a polycarbonate membrane (0.4 μm, Merck). Every 48 h, each Petri dish was sectioned into seven quadrants of 6.25 cm^2; the biomass from each section was carefully separated from the membrane using a spatula and used to prepare crude enzyme extracts.

2.4.7 *Crude enzyme extracts (CEE)*

Approximately 100 mg of fresh biomass were ground in liquid nitrogen and homogenized in 1 mL of sodium phosphate buffer (50 mM, pH 7) containing 5 μL of a protease inhibitor cocktail (P2714, Sigma). The

homogenates were centrifuged (14000 rpm, 4 °C, 15 min), and the resulting supernatants were designated as CEE. Enzymatic activities in the CEE were quantified spectrophotometrically as described below. Protein concentration in the CEE was determined at 595 nm using the Bradford method (Bradford, 1976), with a commercial kit (500-0006, Bio-Rad) and bovine serum albumin (A-7906, Sigma-Aldrich) as the standard (0–10 mg L^{-1}).

2.4.8 Superoxide dismutase (SOD, EC 1.15.1.1)

Superoxide dismutase (SOD) activity was quantified using the method of Beyer and Fridovich (1987). One mL of a mixture prepared with nitro-blue tetrazolium (NBT 110 μM), Triton X-100 (0.05%), and EDTA (4 mM) was added with 30 μL of CEE. The mixture was added with 20 μL of riboflavin (1 mM) and 1 mL of L-methionine (20 mM). In the blank, CEE was replaced by phosphate buffer (50 mM, pH 7). The mixture was incubated for 10 min at room temperature, and absorbance was measured at 560 nm. One unit of SOD activity is defined as the amount of enzyme required to inhibit NBT reduction by 50% at 26°C and pH 6.5.

2.4.9 Catalase (CAT, EC 1.11.1.6)

Catalase (CAT) activity was determined using the method of Aebi (1984). The CEE (200 μL) was mixed with 1 mL of 20 mM H_2O_2 in sodium phosphate buffer (50 mM, pH 7.0). In the blank, H_2O_2 was replaced by the same buffer. Enzyme activity was determined by measuring the decrease in absorbance at 240 nm every 30 s for 5 min, using a molar extinction coefficient (ε) of 39.4 mM^{-1} cm^{-1} (Aebi 1984). One unit of CAT activity is defined as the amount of enzyme required to decompose 1 μmol of H_2O_2 per minute at 26°C and pH 7.

2.4.10 Peroxidases (G-POX, EC 1.11.1.7)

Guaiacol peroxidase (G-POX) activity was determined according to the method of Kim and Yoo (1996). The CEE (100 μL) was mixed with 780 μL of sodium phosphate buffer (50 mM, pH 7.0) and 80 μL of H_2O_2 (20 mM); in the blank, H_2O_2 was replaced by phosphate buffer. The reaction was started by adding 40 μL of guaiacol (1%, v/v), and the increase in absorbance at 450 nm was recorded every 30 s for 5 min. The activity was calculated using a ε of 26.6 mM^{-1} cm^{-1} (Chance and Maehly, 1955). One unit of G-POX activity is defined as the amount of enzyme that catalyzes the formation of 1 μmol of tetraguaiacol per minute at 26 °C and pH 7.

2.4.11 Statistical analysis

Data obtained from the CCD were analyzed by ANOVA. Pearson's correlation coefficients were calculated to test the linear relationship among dependent variables. Data were tested by one-way ANOVA, and the comparison of the means was done using a Tukey test (α = 0.05). Results are presented as mean ± standard deviation (SD), and statistically significant differences are indicated by different letters. Statistical analyses were conducted using SAS (version 9.1.3, SAS Institute Inc.) and STATISTICA (version 7.0, USA) software.

3 Results and discussion

3.1 Dextrose and CuO-NP effect on growth and copper sorption

Different concentrations of dextrose and CuO-NPs were evaluated to establish the optimal experimental conditions for subsequent assays. The results of biomass, melanin and Cu sorption (Table S1) obtained from the CCD were analyzed by ANOVA. The analysis identified the variables that significantly influence these three responses in *Cladosporium* sp. UAM12. Based on the corresponding ANOVA (Tables S2, S3 and S4) for each response variable, three second-order equations for Cu sorption (Eq. 3), melanin production (Eq. 4), and biomass production (Eq. 5) were obtained:

$$Cu(mg\ g^{-1}) = 4.181 - 0.063x_1 + 0.716x_2 - 0.190x_1x_2 - 0.478\ x_1^2 - 0.042\ x_2^2 \quad (3)$$

$$Melanin(mg\ g^{-1}) = 1.581 + 1.120x_1 - 0.015x_2 - 0.223x_1x_2 + 0.085\ x_1^2 + 0.522\ x_2^2 \quad (4)$$

$$Biomass(mg) = 132.777 + 22.215x_1 - 13.478x_2 - 15.025x_1x_2 - 20.027\ x_1^2 - 2.222\ x_2^2 \quad (5)$$

Where x_1 and x_2 are the encoded values for dextrose and CuO-NPs concentration, respectively; x_1x_2 represents the interaction between both variables; x_1^2 and x_2^2 correspond to the quadratic effects of dextrose and CuO-NPs, respectively. The coefficients of determination for equations 3 (R^2= 0.984), 4 (R^2= 0.973), and 5 (R^2= 0.955) indicate strong agreement between the predicted and experimental values. These results confirm the reliability of the models for describing trends in the three variables. Although the interaction term (x_1x_2) and the quadratic term (x_2^2) in the melanin production model did not show statistically significant effects ($p > 0.05$), they were maintained in the equation because their contribution to a good fit of the quadratic model prediction (R^2 = 0.973). This allowed a more accurate description of melanin production behavior, considering the possible combined effects and the nonlinear relationship

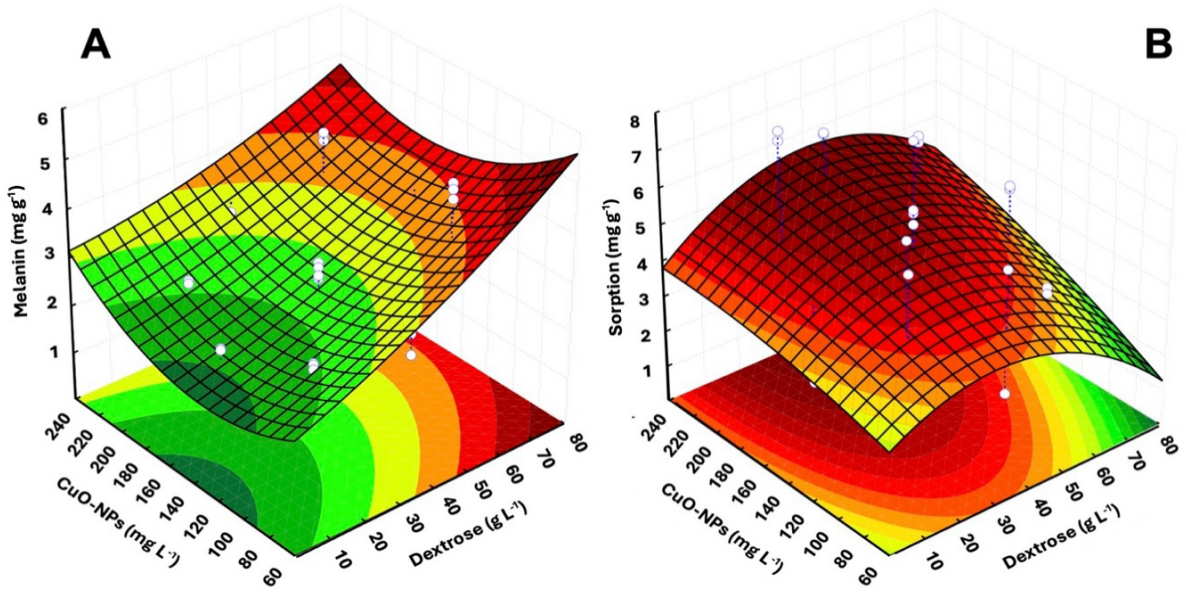

Figure 1. Response surface plots predicting melanin production **(A)** and Cu sorption **(B)** by *Cladosporium* sp. UAM12 as a function of initial CuO-NPs and dextrose concentrations.

between the evaluated variables (dextrose and CuO-NPs) within the experimental range. Although the biomass model (Eq. 5) was satisfactory, melanin synthesis and Cu sorption are the primary mechanisms enabling *Cladosporium* sp. to tolerate CuO-NPs. Therefore, these two responses were prioritized to define and optimize the experimental conditions, and Eqs. 3 and 4 were used to generate the response surface curves shown in Fig. 1.

For melanin production (Fig. 1A), the response surface showed an ascending ridge, indicating that dextrose concentration was the only independent variable with a statistically significant linear effect ($p < 0.05$), while interaction and quadratic terms were retained to accurately plot the response surface. In contrast, the response surface for Cu sorption (Fig. 1B) also exhibited an ascending trend, with CuO-NPs concentration identified as the factor significantly influencing this response. The canonical analysis allowed to identify CuO-NP and dextrose concentrations that enhance both melanin production and Cu sorption.

For sorption, the model predicted that supplementing the medium with 210 mg L^{-1} CuO-NPs and 35 g L^{-1} dextrose would yield 5.06 mg g^{-1} biomass. However, the tolerance curve showed that 200 mg L^{-1} CuO-NPs inhibited fungal growth by 50% at this dextrose concentration, indicating that the predicted optimal sorption may compromise fungal viability. For melanin, the canonical analysis suggested that 160 mg L^{-1} CuO-NPs combined with 60 g L^{-1} dextrose increased production 3.7-fold compared to controls (1.39 ± 0.19 mg g^{-1} biomass). Similarly, a fractional factorial design in *A. nidulans* showed that increasing glucose concentration from 10 to 16 g L^{-1} enhanced melanin production 2.3-fold (Campanhol *et al*., 2023), confirming the positive effect of carbon availability on pigment biosynthesis. Experimental validation further supported that carbon source concentration significantly influences pigment synthesis, including melanin, consistent with previous findings (Sun *et al*., 2016). The results also indicate that melanin content in *Cladosporium* sp. hyphae correlates with Cu sorption. It should be noted that increased fungal growth does not necessarily lead to higher pigment yields, as melanin is a secondary metabolite synthesized during the late growth phase (Suthar *et al*., 2023).

3.2 Effect of dextrose on CuO-NP tolerance and melanin production

The conditions predicted by the CCD were experimentally validated by independent experiments conducted outside the original experimental design range, varying the concentration of dextrose (20, 40 and 60 g L^{-1}) and CuO-NPs (0–300 mg L^{-1}). Results in Sabouraud medium supplemented with dextrose showed that both dextrose and CuO-NPs concentration significantly influenced biomass and melanin production in *Cladosporium* sp. (Fig. 2). The model predicted that 80 mg L^{-1} CuO-NPs combined with 56 g L^{-1} dextrose would yield 170 mg of biomass. However, the tolerance curve at 60 g L^{-1} dextrose revealed that 70 mg L^{-1} CuO-NPs reduces biomass by 29.5%. Conversely, the NP concentration optimized for melanin synthesis (160 mg L^{-1}) did not inhibit growth by ≥50%, regardless of dextrose concentration. Thus, precise CuO-NP concentration definition is critical for evaluating their toxic effects

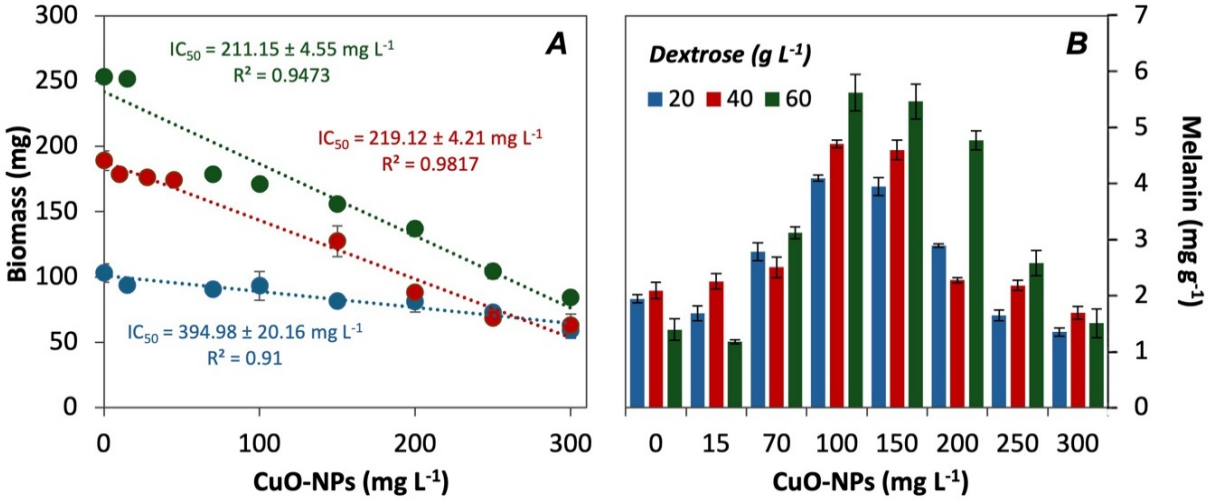

Figure 2. **(A)** Half inhibitory concentration (IC_{50}) for CuO-NPs and **(B)** melanin production by *Cladosporium* sp. UAM12 after 14 days at 27 °C, as a function of initial CuO-NPs and dextrose concentrations.

and detoxification mechanisms without compromising fungal growth. The results revealed a dose-dependent interaction between carbon availability, melanin synthesis, and CuO-NP tolerance (Fig. 2). Contrary to the hypothesis that high carbon concentrations would strengthen stress responses, increasing dextrose to 40 and 60 g L^{-1} resulted in a reduced tolerance to CuO-NPs, decreasing the IC_{50} to values near 200 mg L^{-1} (Fig. 2A). In contrast, with 60 g L^{-1} dextrose, melanin accumulation increased significantly in the presence of NP within a range of 100–200 mg L^{-1}, reaching maximum production at 100 and 150 mg L^{-1} CuO-NP (Fig. 2B). Based on these results, further assays were conducted using 60 g L^{-1} dextrose and 160 mg L^{-1} CuO-NPs.

The decreased tolerance to CuO-NPs in the presence of high dextrose concentrations could be attributed either to increased oxidative stress or to catabolite repression (Yu *et al*., 2026). As previously reported, high glucose availability can increase glucose oxidase activity, leading to the accumulation of H_2O_2 (Wang *et al*., 2006; Salgado-Bautista *et al*., 2020). Consequently, simultaneous exposure to high dextrose concentrations and CuO-NPs could subject *Cladosporium* sp. UAM12 to a greater ROS accumulation, overloading its basal antioxidant defenses. The above suggests that, to counteract this double stress, the fungus may be redirecting its biochemical machinery towards melanin biosynthesis.

Although melanin is not essential for primary growth, it acts as a key protective barrier against oxidative damage (Lin and Xu, 2023). This mechanism aligns with the behavior observed in other tolerant microorganisms, where biomass components and surface structures play a fundamental role in the adsorption and sequestration of HM to prevent intracellular damage (Cabrales-González *et al*., 2022). This structural defense is evidenced by the maximum accumulation of melanin with 60 g L^{-1} dextrose combined with 100–150 mg L^{-1} CuO-NPs. It is noteworthy that, despite the reduction in IC_{50} with high dextrose concentrations, the tolerance of *Cladosporium* sp. UAM12 remains high compared to other fungi. For instance, 50 mg L^{-1} Ag-NPs caused severe growth inhibition (70–90%) in *Cladosporium cladosporoides* and *Aspergillus niger* (Pulit *et al*., 2013), and 38 mg L^{-1} CuO-NPs inhibited 90% of growth in *Candida albicans* (García-Marin *et al*., 2022). In contrast, the optimized condition (160 mg L^{-1} CuO-NPs) found in this study allowed both high growth and NP detoxification. This highlights the high efficiency of melanin-mediated copper sequestration in the cell wall and the antioxidant enzyme responses triggered in this DSE.

3.3 Growth and adaptive response of Cladosporium sp. to CuO-NPs

Kinetic assays were conducted in the presence of 160 mg L^{-1} CuO-NPs to assess the adaptation and tolerance of *Cladosporium* sp. under moderate stress (below IC_{50}). The NPs (≤50 nm) contain approximately 62% copper, of which about 36% is soluble in the culture medium (pH ~5.5). No significant differences in biomass production were recorded, with maximum values reached with or without CuO-NPs after 10 days of culture (Fig. 3A). However, NPs induced a delay in dextrose consumption between 2 and 12 days, with a rate of 4.26 ± 0.15 mg mL^{-1} day^{-1} compared to 5.63 ± 0.44 mg mL^{-1} day^{-1} in the control (0–10 days). Despite this delay, no significant differences were found in total dextrose consumption (~88%) after 14 days. At the end of the culture, melanin synthesis increased 1.6-

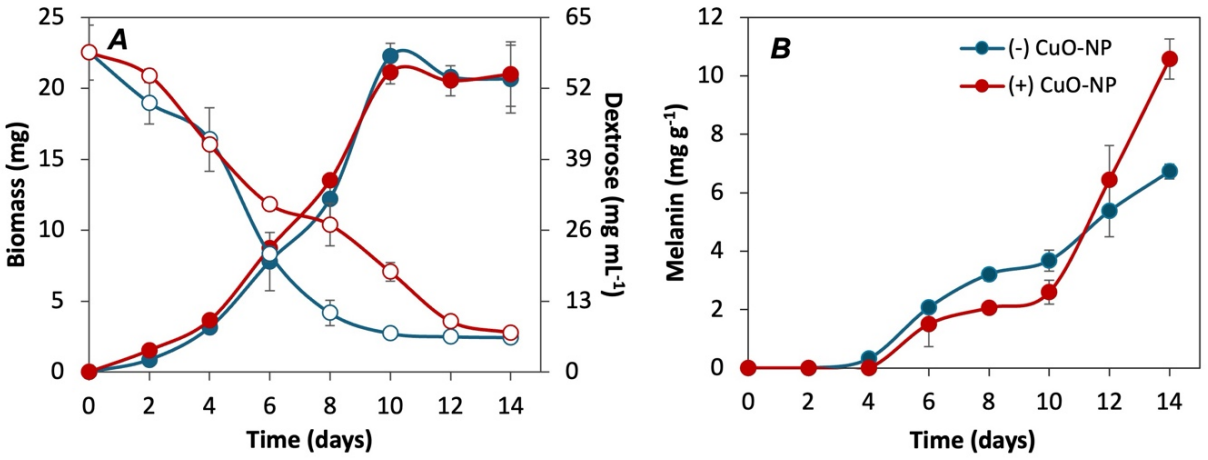

Figure 3. **(A)** Biomass production (filled circles) and dextrose consumption (open circles), and **(B)** melanin synthesis by *Cladosporium* sp. UAM12 grown for 14 days in the absence (–) and presence (+) of CuO-NPs (160 mg L^{-1}).

Table 1. Specific growth rate (μ), doubling time (t_d) and cell yield (Y_{XS}) of 14-day cultures of *Cladosporium* sp. without (–) and with (+) CuO-NPs (160 mg L^{-1}). *

Treatment	μ (day^{-1})	t_d (days)	Y_{XS} (mg mg^{-1})
(–) CuO-NPs	0.410 ± 0.017[a]	1.69 ± 0.07[b]	0.48 ± 0.03[a]
(+) CuO-NPs	0.328 ± 0.009[b]	2.11 ± 0.06[a]	0.52 ± 0.03[a]

*Data with different letters by column indicate significant differences ($p < 0.001$). Values correspond to the mean value of three replicates ± standard deviation values.

fold in the presence of NPs compared to controls (6.73 ± 0.24 mg g^{-1} biomass). Whereas melanin production in the control proceeded at a constant rate from 4 to 14 days (0.59 ± 0.01 mg g^{-1} day^{-1}), cultures exposed to CuO-NPs exhibited two different phases: a slow phase from 4 to 10 days (0.42 ± 0.05 mg g^{-1} day^{-1}) followed by a rapid phase from 10 to 14 days (2.00 ± 0.15 mg g^{-1} day^{-1}) (Fig. 3B).

Based on the growth and substrate consumption kinetics, the specific growth rate (μ), doubling time (t_d), and the final cell yield (Y_{XS}) of *Cladosporium* sp. were estimated (Table 1). The presence of CuO-NPs reduced μ by 19.9%, resulting in a 10.1 h (0.42 days) increase in t_d. Nevertheless, the final Y_{XS} value did not differ significantly between treatments. The fact that there were no significant differences in biomass production because of CuO-NPs indicates that *Cladosporium* sp. tolerates moderate stress conditions. The delay in dextrose consumption observed between 2 and 12 days is consistent with the gradual release of Cu^{2+} ions into the medium. Since the amount of Cu^{2+} released is directly related to the initial NP concentration, the delay in dextrose consumption could reflect the progressive ion accumulation in the mycelium (Singh *et al*., 2021).

Despite the growth delay, the fungus overcame copper stress after 12 days, coinciding with a marked increase in melanin synthesis. Similar responses have been reported in other DSE fungi. For example, *E. pisciphila* exposed to 150 mg L^{-1} Cd^{2+} showed a 1.3-fold increase in melanin production compared to metal-free cultures (Zhan *et al*., 2011). *Gaeumannomyces cylindrosporus* accumulated 5.2-fold more melanin under Pb^{2+} stress compared to controls (1.8 mg g^{-1} biomass) (Ban *et al*., 2012). These findings, together with the present study, reinforce the role of melanin as a defense mechanism against HM-induced stress, acting as a physical barrier that limits toxicity (Juárez-Maldonado *et al*., 2021).

3.4 *Melanin and the control of oxidative stress*

Copper was solubilized from CuO NPs in Sabouraud medium at a rate of 17.08 ± 0.15 mg L^{-1} day^{-1}, directly influencing the sorption by *Cladosporium* sp. Over 14 days, the fungus accumulated up to 3.18 ± 0.55 mg g^{-1} biomass, with 80.1 ± 4.9% immobilized in the cell wall. Furthermore, melanin production was inhibited by kojic acid but not by tricyclazole (data not shown), indicating that *Cladosporium* sp. UAM12 primarily synthesizes DOPA-melanin (a type of eumelanin). Similarly, Buszman *et al*. (2006) identified mainly eumelanin in *C. cladosporioides* and identified only a small proportion of pheomelanin. This type of melanin is synthesized via the L-DOPA pathway, which uses tyrosine as a precursor, and kojic acid inhibits the synthesis by blocking the formation of

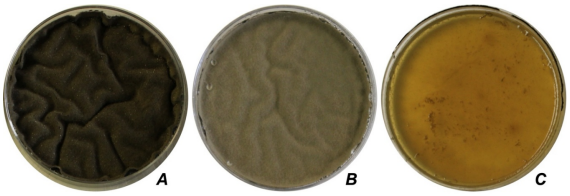

Figure 4. Effect of kojic acid (3 g L^{-1}) on melanin synthesis inhibition in *Cladosporium* sp. after 14 days of culture in Sabouraud medium containing 60 g L^{-1} dextrose. **(A)** Control without kojic acid; **(B)** culture with kojic acid; **(C)** culture with kojic acid and CuO-NPs (160 mg L^{-1}).

5,6-dihydroxyindole-2-carboxylic acid by tyrosinase (Berthelot *et al*., 2020; Suthar *et al*., 2023).

Kojic acid (3 g L^{-1}) reduced melanin production in *Cladosporium* sp. UAM12 by ~26% (4.62 ± 0.20 vs. 6.26 ± 0.27 mg g^{-1} biomass in controls) without affecting growth, shifting pigmentation from brownish-black to brownish-green, thereby confirming reduced melanin synthesis (Fig. 4). Under these conditions, exposure to 160 mg L^{-1} CuO NPs suppressed biomass by ~95%, highlighting the protective role of DOPA-melanin. The recovery of *Cladosporium* sp. from copper toxicity (Fig. 3A) is likely associated with the immobilization of ~80% of the accumulated metal in the cell wall, where melanin plays a key protective role. This suggests that enhanced melanin content in the cell wall restricts intracellular bioaccumulation of Cu^{2+} ions released during 14 days of culture, thereby mitigating toxicity and conferring an adaptive advantage (Suthar *et al*., 2023).

The heavy metal sorption capacity of melanized fungi is highly dependent on the complex physicochemical properties of eumelanin. Its chemical structure includes indole rings, quinones, carboxylates, and amides, as well as a paramagnetic center generated by homogeneously distributed *o*-semiquinone radicals (Singh *et al*., 2021). These free radicals significantly enhance the melanin affinity for metal ions by enabling a diverse array of chemical and magnetic interactions. For instance, in *C. cladosporioides*, both magnetic and chemical interactions between eumelanin free radicals and Cu^{2+} ions have been observed (Buszman *et al*., 2006). These interactions effectively sequester Cu^{2+} ions within the fungal cell wall, thereby reducing intracellular accumulation and conferring tolerance against stress induced by MNP. This cell wall retention mechanism is consistent with our results and similar findings in *Exophiala salmonis* exposed to 150 mg L^{-1} CuO-NPs, where 91.1% of the accumulated Cu (~1.80 mg g^{-1}) was retained in the cell wall (Ban *et al*., 2023). Furthermore, the strong positive correlation (Pearson = 0.932) observed between melanin production and Cu sorption in a range of CuO-NP concentrations (15–150 mg L^{-1}; Fig. S1) further supports that melanin-mediated sequestration is fundamental to fungal tolerance under MNP stress.

Since melanin plays a key role in limiting the entry of Cu^{2+} ions into the cell, its inhibition also reduces fungal tolerance to CuO-NPs. This effect was observed in *Cladosporium* sp. UAM12 cultures exposed to 160 mg L^{-1} CuO-NPs in the presence of kojic acid, where growth was almost completely inhibited (Fig. 4C). Similar trends have been reported in other DSE fungi, where the inhibition of melanin synthesis decreases tolerance to HMs (Berthelot *et al*., 2020; Potisek *et al*., 2021). However, a recent study on six DSEs showed that melanin inhibition did not significantly affect Cd or Zn tolerance but altered the pattern of metal accumulation (Berthelot *et al*., 2020). Increased intracellular metal uptake leads to ROS overproduction, which, if not controlled, reduces fungal tolerance (Potisek *et al*., 2021). In this study, the severe growth inhibition of *Cladosporium* sp. UAM12 in the presence of CuO-NPs and kojic acid confirms that Cu tolerance in this strain is strongly dependent on melanin synthesis. The above could be directly related to the role of melanin as a first-line defense mechanism by binding Cu to the cell wall, thereby preventing its intracellular accumulation and reducing metal toxicity.

3.5 Antioxidant response in Cladosporium sp.

Superoxide dismutase (SOD) and G-POX activity in *Cladosporium* sp. were significantly stimulated in the presence of CuO-NPs (Fig. 5); SOD activity reached a maximum level (14.5-fold higher than the control) after 6 days (Fig. 5A), whereas G-POX activity had a maximum (3.3-fold above the control) after 12 days of culture (Fig. 5B). CAT activity showed a significant increase (1.8-fold) only after 14 days and exhibited a gradual rise independent of the presence of NPs (Fig. 5C). Once a fraction of Cu enters the cell (19.9 ± 4.9% in this study), the inevitable consequence is the overproduction of ROS, leading to redox imbalance; if uncontrolled, this imbalance culminates in oxidative stress (Ban *et al*., 2023). Antioxidant enzymes such as SOD, G-POX, and CAT play central roles in mitigating ROS damage, and their increased activity in *Cladosporium* sp. UAM12 reflects an adaptive tolerance mechanism (Potisek *et al*., 2021). The upregulation of these enzymes underscores their role in mitigating the effects of intracellular Cu^{2+} ions (~0.63 mg g^{-1} biomass, based on cell wall retention).

Pollutants such as MNPs, often undergo redox cycling, generating free radicals and ROS through successive oxidation–reduction reactions. These radicals readily react with O_2, generating $\cdot O_2^-$ and other ROS (Peralta-Pérez and Volke-Sepúlveda,

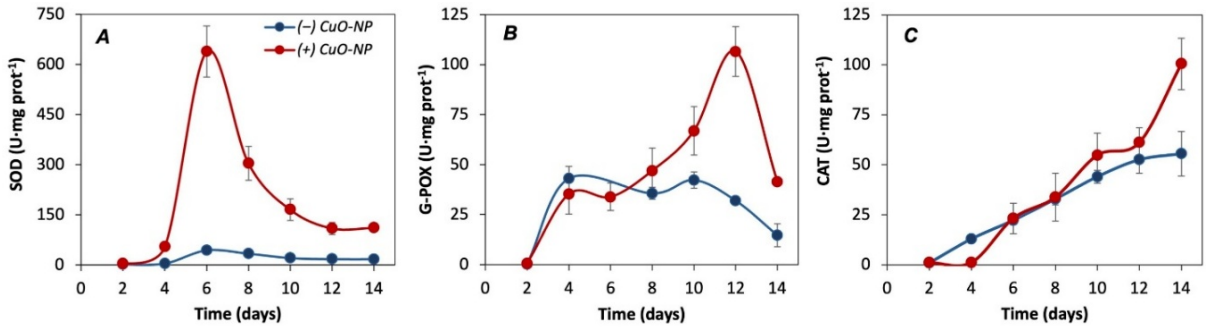

Figure 5. Specific activities of **(A)** superoxide dismutase (SOD), **(B)** peroxidase (G-POX), and **(C)** catalase (CAT) in *Cladosporium* sp. UAM12 after 14 days of growth in the absence (–) and presence (+) of CuO-NPs (160 mg L^{-1}).

2012). The early increase in SOD activity (during the first 6 days) in cultures exposed to CuO-NPs confirms that this enzyme serves as a primary defense mechanism in *Cladosporium* sp. by regulating $\cdot O_2^-$ levels and counteracting Cu^{2+} induced oxidative stress. From the sixth day onward, melanin synthesis increased while SOD activity declined, resulting in a strong negative correlation between both parameters in the presence of 160 mg L^{-1} CuO-NPs (Fig. S2). A pronounced decrease in SOD activity was found when melanin levels rose from 1.3 to 2.6 mg g^{-1} biomass (Pearson = -0.950), followed by a slower decline as melanin increased from 2.6 to 10.8 mg g^{-1} (Pearson = -0.807). The most significant reduction in SOD activity (Fig. 5A) coincided with the period of accelerated melanin production (10–14 days) (Fig. 3B), supporting the idea that melanin progressively plays a predominant antioxidant role, limiting Cu^{2+} uptake and alleviating intracellular stress. Comparable responses have been reported in *Acrocalymma vagum* and *Scytalidium lignicola* exposed to Cd^{2+} (Hou *et al*., 2020), and *G. cylindrosporus* under Pb^{2+}exposure (Ban *et al*., 2012).

As the dismutation of $\cdot O_2^-$ by SOD generates H_2O_2, this ROS must be further degraded to by catalase and peroxidases to prevent ·OH formation via the metal-catalyzed Fenton reaction, thereby avoiding oxidative stress (Peralta-Pérez and Volke-Sepúlveda, 2012). The increased G-POX activity found under NP-induced stress suggests that *Cladosporium* sp. can effectively regulate cellular redox balance. Notably, a marked rise in CAT activity compared to the control coincided with a decline in G-POX activity after 12 days (Fig. 5C). This shift may be explained by the low affinity of CAT for H_2O_2, so this enzyme removes high concentrations of H_2O_2 (in the mM range). At such levels, CAT rapidly decomposes H_2O_2 due to its ability to function as both hydrogen donor and acceptor (Vega-García *et al*., 2018; Potisek *et al*., 2021). This increase in CAT activity could therefore result from enhanced H_2O_2 accumulation resulting from prolonged exposure of the mycelium to Cu^{2+} ions, suggesting a protective mechanism against ROS-induced damage. Peroxidases exhibit higher affinity for H_2O_2 than CAT, typically in the micromolar range (Vega-García *et al*., 2018). In particular, G-POX plays a central role in H_2O_2 detoxification under both normal and stress conditions, due to its relatively high activity in intracellular, extracellular, and cell wall compartments. The induction of this enzyme has been widely reported under environmental stress, including HMs (Zandi and Schnug, 2022). For instance, *E. salmonis* exposed to 150 mg L^{-1} CuO-NPs showed 2.7- and 4.5-fold increases in SOD and peroxidase activities, respectively, compared with controls (Ban *et al*., 2023). Similarly, increased CAT activity has been observed in fungi exposed to HM, such as *G. cylindrosporus* treated with Pb^{2+} (Ban *et al*., 2012) and *Cadophora* sp. under Cd^{2+} stress (Potisek *et al*., 2021).

Collectively, our findings help to elucidate the mechanisms underlying the high tolerance of *Cladosporium* sp. UAM12 to CuO-NPs, demonstrating a synergistic action between melanin accumulation and antioxidant enzyme activity. Melanin plays a key role in mitigating oxidative stress by immobilizing Cu^{2+} within the fungal cell wall, thereby preventing excessive ROS formation. At the same time, the upregulation of antioxidant enzymes, particularly SOD and G-POX, acts as an adaptive response against oxidative stress. Although further studies on the antioxidant system of this strain are required –given that ROS production can vary depending on nanoparticle properties and culture conditions– understanding these physiological strategies provides a basis for using this fungus in environmental applications.

Furthermore, the ability of *Cladosporium* sp. UAM12 to effectively sequester Cu^{2+} ions offers a promising prospect for the development of bioremediation systems. The fungal biomass could be used as a biosorbent material for the removal of HM from contaminated liquid effluents, employing fixed-bed columns or stirred-tank bioreactors. In addition to engineered bioremediation, the ecological nature of *Cladosporium* sp. UAM12 as a DSE fungus highlights

its potential for endophyte-assisted phytoremediation. DSE colonization enhances the plant growth and immobilizes metal ions within the fungal hyphae, creating physical barriers that protect the host plant (Cao *et al*., 2023). Given that *Cladosporium* sp. UAM12 was isolated from *Dodonaea viscosa* – where it significantly enhances the plant growth under lead stress, partly by mitigating oxidative damage (unpublished data)– this strain represents a highly viable candidate for remediating contaminated agricultural soils. Based on its antioxidant defense and melanin-mediated metal retention, the application of this DSE fungus could be a valuable strategy to increase crop productivity while simultaneously minimizing the transfer of HM and MNPs into the food chain.

Conclusions

This study demonstrates that, although high dextrose availability stimulates biomass yield and DOPA-melanin synthesis in *Cladosporium* sp. UAM12, it also reduces tolerance to CuO-NPs due to the likely combination of dextrose-induced endogenous oxidative stress with NP toxicity. However, optimizing these variables (60 g L^{-1} dextrose and 160 mg L^{-1} CuO-NPs) allows for the activation of an efficient defense mechanism. Under these specific conditions, melanin accumulation acts synergistically with antioxidant enzymes, particularly superoxide dismutase and peroxidases, to sequester most of the soluble copper in the cell wall and mitigate oxidative damage. These physiological mechanisms confer upon *Cladosporium* sp. UAM12 a high tolerance to CuO-NPs compared to other DSE fungi, highlighting the importance of an adequate nutritional balance when using this type of fungi for the bio- or phytoremediation of environments contaminated with metallic NPs.

Acknowledgements

M.E. Contla-Ubaldo thanks the Secretariat of Science, Humanities, Technology and Innovation (SECIHTI) for granting his Ph.D. scholarship (grant number 815063).

References

Aebi H. (1984). Catalase in vitro. *Methods in Enzymology*. 105, 121-126. https://doi.org/10.1016/S0076-6879(84)05016-3

Ban Y, Tang M, Chen H, Xu Z, Zhang H, Yang Y. (2012). The response of dark septate endophytes (DSE) to heavy metals in pure culture. *PLoS ONE*. 7, 47968. https://doi.org/10.1371/journal.pone.0047968

Ban Y, Tan J, Xiong Y, Mo X, Li W, Jia C, Xu Z. (2023). The responses and detoxification mechanisms of dark septate endophytes (DSE), *Exophiala salmonis*, to CuO nanoparticles. *Environmental Science and Pollution Research.* 30, 13773-13787. https://doi.org/10.1007/s11356-022-23099-1

Beltrán-García MJ, Prado FM, Oliveira MS, Ortiz-Mendoza D, Scalfo AC, Pessoa Jr A, Di Mascio P. (2014). Singlet molecular oxygen generation by light-activated DHN-melanin of the fungal pathogen *Mycosphaerella fijiensis* in black Sigatoka disease of bananas. *PLoS ONE*. 9, e91616. https://doi.org/10.1371/journal.pone.0091616

Berthelot C, Zegeye A, Gaber DA, Chalot M, Franken P, Kovács GM, Blaudez D. (2020). Unravelling the role of melanin in Cd and Zn tolerance and accumulation of three dark septate endophytic species. *Microorganisms.* 8, 537. https://doi.org/10.3390/ microorganisms8040537

Beyer Jr WF, Fridovich I. (1987). Assaying for superoxide dismutase activity: some large consequences of minor changes in conditions. *Analytical Biochemistry.* 161, 559-566. https://doi.org/10.1016/0003-2697(87)90489-1

Bradford MM. (1976). A rapid and sensitive method for the quantitation of microgram quantities of protein utilizing the principle of protein-dye binding. *Analytical Biochemistry Journal.* 72, 248-254. https://doi.org/10.1016/0003-2697(76)90527-3.

Buszman E, Pilawa B, Zdybel M, Wilczynski S, Gondzik A, Witoszynska T, Wilczok T. (2006). EPR examination of Zn^{2+} and Cu^{2+} binding by pigmented soil fungi *Cladosporium cladosporioides*. *Science of the Total Environment*. 363, 195–205. https://doi.org/10.1016/j.scitotenv.2005.05.028

Cabrales-González AM, Martínez-Prado MA, Núñez-Ramírez DM, Meléndez-Sánchez ER, Medina-Torres L, Parra-Saldivar R. (2022). Bioleaching of As from mine tailings using an autochthonous *Bacillus cereus* strain. *Revista Mexicana de Ingeniería Química*, 21. Bio2723. https://doi.org/10.24275/rmiq/bio2723

Campanhol BS, Ribeiro BD, Casellato F, Medina KJD, Sponchiado SRP. (2023). Improvement of DOPA-melanin production by *Aspergillus nidulans* using eco-friendly and inexpensive substrates. *Journal of Fungi.* 9, 714. https://doi.org/10.3390/jof9070714

Cao G. H., Li X. G., Zhang C. R., Xiong Y. R., Li X., Li T., & Yu J. (2023). Physiological response mechanism of heavy metal-resistant endophytic fungi isolated from the roots of *Polygonatum kingianum*. *Environmental Microbiology Reports*, 15, 568–581. https://doi.org/10.1111/1758-2229.13194

Chance B, Maehly AC. (1955). Assay of catalases and peroxidases. *Methods in Enzymology*, 764-775. https://doi.org/10.1016/S0076-6879(55)02300-8

DuBois M, Gilles KA, Hamilton JK, Rebers PT, Smith F. (1956). Colorimetric method for determination of sugars and related substances. *Analytical Chemistry Journal.* 28, 350-356. https://doi.org/10.1021/ac60111a017

García-Marin LE, Juarez-Moreno K, Vilchis-Nestor AR, Castro-Longoria E. (2022). Highly antifungal activity of biosynthesized copper oxide nanoparticles against *Candida albicans*. *Nanomaterials.* 12, 3856. https://doi.org/10.3390/nano12213856

Hou L, Yu J, Zhao L, He X. (2020). Dark septate endophytes improve the growth and the tolerance of *Medicago sativa* and *Ammopiptanthus mongolicus* under cadmium stress. *Frontiers in Microbiology.* 10, 3061. https://doi.org/10.3389/fmicb.2019.03061

Jimenez-Gonzalez A, Tec-Caamal EN, Medina-Moreno SA. (2024). Biosorption performance evaluation of azo dyes Reactive Red 2 and Reactive Blue 4 on thermally sterilized biomass of *Cladosporium tenuissimum* fungus. *Revista Mexicana de Ingeniería Química*, 23 (1), IA24161. https://doi.org/10.24275/rmiq/IA24161

Juárez-Maldonado A, Tortella G, Rubilar O, Fincheira P, Benavides-Mendoza A. (2021). Biostimulation and toxicity: The magnitude of the impact of nanomaterials in microorganisms and plants. *Journal of Advanced Research.* 31, 113-126. https://doi.org/10.1016/j.jare.2020.12.011

Khan I, Aftab M, Shakir S, Ali M, Qayyum S, Rehman M, Touseef I. (2019). Mycoremediation of heavy metal (Cd and Cr)–polluted soil through indigenous metallotolerant fungal isolates. *Environmental Monitoring and Assessment.* 191, 585. https://doi.org/10.1007/s10661-019-7769-5

Kim YH, Yoo YJ. (1996). Peroxidase production from carrot hairy root cell culture. *Enzyme and Microbial Technology.* 18, 531-535. https://doi.org/10.1016/0141-0229(95)00168-9

Kumar KS, Dahms HU, Won EJ, Lee J, Shin KH. (2015). Microalgae: a promising tool for heavy metal remediation. *Ecotoxicology and Environmental Safety.* 113, 329-352. https://doi.org/10.1016/j.ecoenv.2014.12.019

Lin L, Xu J. (2023). Production of fungal pigments: Molecular processes and their applications. *Journal of Fungi.* 9, 44. https://doi.org/10.3390/jof9010044

Lu H, Wei T, Lou H, Shu X, Chen Q. (2021). A critical review on communication mechanism within plant-endophytic fungi interactions to cope with biotic and abiotic stresses. *Journal of Fungi.* 7, 719. https://doi.org/10.3390/jof7090719

Malicka M, Magurno F, Piotrowska-Seget Z. (2022). Plant association with dark septate endophytes: When the going gets tough (and stressful), the tough fungi get going. *Chemosphere.* 302, 134830. https://doi.org/10.1016/j.chemosphere.2022.134830

Peralta-Pérez MR, Volke-Sepúlveda TL (2012). La defensa antioxidante en las plantas: una herramienta clave para la fitorremediación. *Revista Mexicana de Ingeniería Química*, 11 (1): 75-88

Potisek M, Likar M, Vogel-Mikuš K, Arčon I, Grdadolnik J, Regvar M. (2021). 1,8-dihydroxy naphthalene (DHN)-melanin confers tolerance to cadmium in isolates of melanised dark septate endophytes. *Ecotoxicology and Environmental Safety.* 222, 112493. https://doi.org/10.1016/j.ecoenv.2021.112493

Priyadarshini E, Priyadarshini SS, Cousins BG, Pradhan N. (2021). Metal-Fungus interaction: Review on cellular processes underlying heavy metal detoxification and synthesis of metal nanoparticles. *Chemosphere.* 274, 129976. https://doi.org/10.1016/j.chemosphere.2021.129976

Pulit J, Banach M, Szczygłowska R, Bryk M. (2013). Nanosilver against fungi. Silver nanoparticles as an effective biocidal factor. *Acta Biochimica*

Polonica. 60, 795-798. https://doi.org/10.18388/abp.2013_2060

Răut I, Călin M, Capră L, Gurban AM, Doni M, Radu N, Jecu L. (2021). *Cladosporium* sp. isolate as fungal plant growth promoting agent. *Agronomy*. 11, 392. https://doi.org/10.3390/agronomy11020392

Saleem MH, Ejaz U, Vithanage M, Bolan N, Siddique KH. (2024). Synthesis, characterization, and advanced sustainable applications of copper oxide nanoparticles: a review. *Clean Technologies and Environmental Policy*. 27, 5719–5744. https://doi.org/10.1007/s10098-024-02774-6

Salgado-Bautista D, Volke-Sepúlveda T, Figueroa-Martínez F, Carrasco-Navarro U, Chagolla-López A, Favela-Torres E. (2020). Solid-state fermentation increases secretome complexity in *Aspergillus brasiliensis*. *Fungal Biology*. 124(8), 723-734. https://doi.org/10.1016/j.funbio.2020.04.006

Singh S, Nimse SB, Mathew DE, Dhimmar A, Sahastrabudhe H, Gajjar A, Shinde PB. (2021). Microbial melanin: Recent advances in biosynthesis, extraction, characterization, and applications. *Biotechnology Advances*. 53, 107773. https://doi.org/10.1016/j.biotechadv.2021.107773

Sun S, Zhang X, Sun S, Zhang L, Shan S, Zhu H. (2016). Production of natural melanin by *Auricularia auricula* and study on its molecular structure. *Food Chemistry*. 190, 801-807. https://doi.org/10.1016/j.foodchem.2015.06.042

Suthar M, Dufossé L, Singh SK. (2023). The enigmatic world of fungal melanin: A Comprehensive Review. *Journal of Fungi*, 9, 891. https://doi.org/10.3390/jof9090891

Tripathi G, Javed Z, Dashora K. (2024). Toxicity of copper oxide nanoparticles on agriculturally important soil rhizobacteria *Bacillus megaterium*. *Emerging Contaminants*. 10, 100280. https://doi.org/10.1016/j.emcon.2023.100280

Vega-García V, Díaz-Vilchis A, Saucedo-Vázquez JP, Solano-Peralta A, Rudiño-Piñera E, Hansberg W. (2018). Structure, kinetics, molecular and redox properties of a cytosolic and developmentally regulated fungal catalase-peroxidase. *Archives of Biochemistry and Biophysics*. 640, 17-26. https://doi.org/10.1016/j.abb.2017.12.021

Wang ZS, Gu YX, Yuan QS. (2006). Effect of nutrition factors on the synthesis of superoxide dismutase, catalase, and membrane lipid peroxide levels in *Cordyceps militaris* mycelium. *Current Microbiology*. 52, 74-79. https://doi.org/10.1007/s00284-005-0193-9

Yu X, Li W, Deng J, He J, Yang C, Lin Q, Bai J, Cao Q. (2026). Strategies for enhancing melanin biosynthesis for industrial scale. *Journal of Agricultural and Food Chemistry,* 74, 13418-13433. https://doi.org/10.1021/acs.jafc.6c01353

Zandi P, Schnug E. (2022). Reactive oxygen species, antioxidant responses and implications from a microbial modulation perspective. *Biology*. 11, 155. https://doi.org/10.3390/ biology11020155

Zhan F, He Y, Zu Y, Li T, Zhao Z. (2011). Characterization of melanin isolated from a dark septate endophyte (DSE), *Exophiala pisciphila*. *World Journal of Microbiology and Biotechnology*. 27, 2483-2489. https://doi.org/10.1007/s11274-011-0712-8

Zhan F, He Y, Li T, Yang YY, Toor GS, Zhao Z. (2015). Tolerance and antioxidant response of a dark septate endophyte (DSE), *Exophiala pisciphila*, to cadmium stress. *Bulletin of Environmental Contamination and Toxicology*. 94(1), 96–102. https://doi.org/10.1007/s00128-014-1401-8